Network models and the interpretation of prolonged infection plateaus in the COVID19 pandemic

Natalia L. Komarova,[1] Asma Azizi,[1] and Dominik Wodarz[2]

[1]Department of Mathematics, University of California Irvine, Irvine, CA 92697

[2] Department of Population Health and Disease Prevention, Program in Public Health, Susan and Henry Samueli College of Health Science, University of California Irvine, Irvine, CA 92697

Abstract

Non-pharmaceutical intervention measures, such as social distancing, have so far been the only means to slow the spread of SARS-CoV-2. In the United States, strict social distancing during the first wave of virus spread has resulted in different types of infection dynamics. In some states, such as New York, extensive infection spread was followed by a pronounced decline of infection levels. In other states, such as California, less infection spread occurred before strict social distancing, and a different pattern was observed. Instead of a pronounced infection decline, a long-lasting plateau is evident, characterized by similar daily new infection levels. Here we show that network models, in which individuals and their social contacts are explicitly tracked, can reproduce the plateau if network connections are cut due to social distancing measures. The reason is that in networks characterized by a 2D spatial structure, infection tends to spread quadratically with time, but as edges are randomly removed, the infection spreads along nearly one-dimensional infection "corridors", resulting in plateau dynamics. Further, we show that plateau dynamics are observed only if interventions start sufficiently early; late intervention leads to a "peak and decay" pattern. Interestingly, the plateau dynamics are predicted to eventually transition into an infection decline phase without any further increase in social distancing measures. Additionally, the models suggest that a second wave becomes significantly less pronounced if social distancing is only relaxed once the dynamics have transitioned to the decline phase. The network models analyzed here allow us to interpret and reconcile different infection dynamics during social distancing observed in various US states.

Introduction

The COVID19 pandemic has caused significant mortality and morbidity around the world [1], and the only means to slow its spread has been the implementation of non-pharmaceutical intervention methods, most notably social distancing [2, 3]. In the United States, stay-home orders have been given and have been implemented to various extents in the different states during the first wave of virus spread, which has resulted in an overall reduction of disease burden [4]. Economic considerations, as well as social distancing fatigue in the population, however, lead to the relaxation of non-pharmaceutical interventions, which has resulted in renewed waves of virus spread across the country.

An interesting characteristic of the dynamics of COVID19 cases during non-pharmaceutical interventions is the different patterns that have been observed across different locations, such as different states / counties in the United States. When strict stay-home orders were put in place and the rate of infection spread slowed down, different dynamics were observed in different locations. In some US states / counties, a pronounced decline of daily COVID19 cases was seen following the onset of strict social distancing. This tends to be the case if infection spread has been more severe, such as in New York (Figure 1a). In other locations, a relatively long-lasting plateau phase was observed, during which the number of daily cases seemed to fluctuate around a steady average level (corresponding to a linear cumulative number of cases over time). This has been seen in places that implemented social distancing measures relatively early and controlled the spread effectively, such as in California or Washington State (Figure 1b).

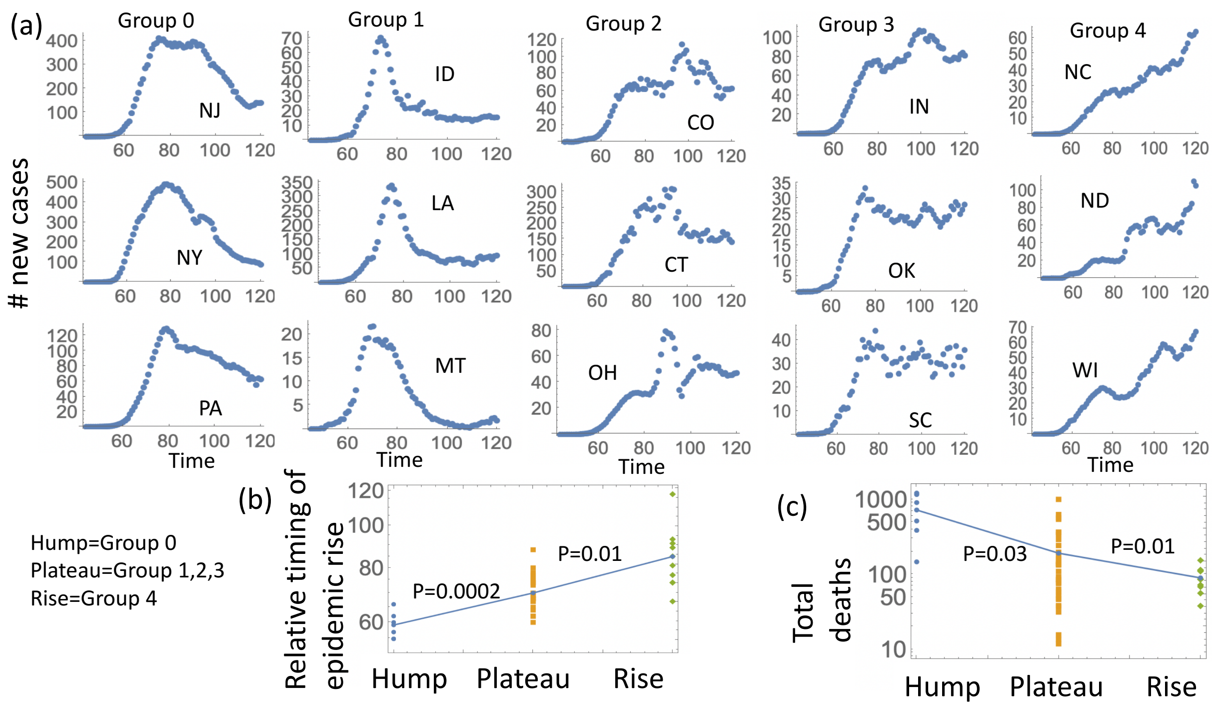

Figure 1: (a) Different patterns of COVID19 spread during social distancing across different states in the USA. Group 0 states show a relatively sharp decline of infections. Group 1 states show an initial decline, followed by convergence to a plateau. Group 2 states show a plateau without a significant decline during social distancing. Group 3 states show a rise, followed by a plateau. Group 4 states show a rise without convergence to a plateau. See Supplementary Materials for grouping methodology. (b) Correlation between the COVID19 spread pattern during social distancing with the relative timing of the epidemic rise (see Supplement Section 3 for details). A later rise of the epidemic is associated with a relatively early implementation of social distancing, which happens before the infection has spread significantly through the population. Thus earlier initiation of distancing correlates with the occurrence of a plateau or even a "rise" (which is thought to correspond to pre-plateau dynamics). Initiation of distancing after significant virus spread tends to correlate with a "hump"-shaped epidemic: a significant infection spread followed by a decline and lack of a plateau. (c) The same trend is seen when considering deaths as an indicator of the severity of infection when distancing is initiated. Less death correlates with the appearance of a plateau or a rise. More death correlates with a sharp rise of infection followed by a decline in the absence of a plateau.

To explain these patterns, this paper analyzes the spread of COVID19 using network models, which assume that individuals in a population do not all mix with each other, but that individuals interact according to contact networks. We assume the existence of contact networks both before and during strict social distancing efforts. Strict social distancing is implemented by cutting these network connections to varying degrees. We find that such models can reproduce the above-described intricacies of COVID19 spread, including the long-lasting infection plateaus observed during strict social distancing. In particular, if strict social distancing is put in place relatively early, the models predict a prolonged plateau phase during which the daily number of infections remains relatively constant. Interestingly, these dynamics transition naturally into a decline phase without any additional cutting of network connections (i.e. without stronger social distancing). In contrast, if strict social distancing measures are implemented only after the infection has spread to higher levels in the model, the plateau phase is less pronounced or absent, and a decline phase is observed right away. Consistent with previous modeling approaches [5, 6], we find that the predicted second wave can be lower if social distancing is relaxed later. In contrast to the predictions from standard SIR models, however, our network models suggest that a lower second wave is only observed if social distancing is relaxed once the steady plateau phase is over and the number of daily new infections has started to decline.

Mathematical models have been useful for obtaining a better understanding of SARS CoV-2 spread dynamics, [7-13]. This has resulted in the estimation of the basic reproduction number [7, 14], in insights into transmission dynamics in the absence and presence of non-pharmaceutical interventions [3, 5, 6, 15-20], and demonstrated the effect of age structure on disease dynamics [16, 21], among a variety of other contributions [10]. A number of mathematical modeling approaches have been explored in this context. Network models, however, have been helpful in studying human behavior in the context of social distancing. In the absence of vaccination, human adaptive reactions or mandated changes that modify interactions on a social network can influence the course of an epidemic [22]. There is a broad theoretical and computational literature on the impact of behavioral changes, such as social distancing, on the patterns of amelioration or prevention of infection spread over social networks [18, 20, 22-28]. Funk et al. [24] and Wu et al. [22] highlighted the importance of risk perception. They studied social distancing via reduction of contacts as awareness flows on the social network, and found that local awareness (self-regulated social distancing decided by individuals due to fear of infection in their neighborhood) in high clustering networks prevents the disease from growing into an epidemic, while global awareness (mandated social distancing imposed by government) is not as effective at controlling infections. A study by Azizi et al. [27] considered coupled infection and awareness dynamics in response to an infection spread, and found a threshold on the level and timing of social distancing which is affected by network structure of human interactions. On the other hand, Leung et al. [26] showed that moderate social distancing that includes a degree of network rewiring can worsen the epidemic outcomes. They demonstrated the crucial impact of network structure on the measures in this context. Using the SIR model on spatial networks, Maharaj et al. [25] conducted efficiency and cost benefit analysis of controlling infection via temporary reduction of contacts by susceptible individuals in response to infection within their local neighborhood. Nishi et al. [28] used network models to study how interventions can be used to counter the spread of SARS CoV-2 while preserving economic activity. They found that two network intervention strategies that divide or balance social groups can reduce infection spread while maintaining significant economic activity.

Our modeling approach adds to this literature, and provides an explanation for patterns of plateau duration and characteristics of subsequent infection waves, in the context of timing, intensity, and duration of social distancing measures.

Using network models to describe the dynamics of epidemics

Network models [29-43] do not assume perfect mixing of individuals, but instead postulate the existence of a graph whose nodes are individuals, and edges represent social contacts through which transmission can occur.

While the true structure of the human contact networks in the absence and presence of the pandemic are not fully understood, we analyzed two basic types of networks at different ends of the spectrum. In what we call a "random spatial network", individuals are connected to their local neighbors; such networks have been extensively studied in the literature, see e.g. [44-47] for general network properties and [29, 48-51] for dynamical processes on random spatial graphs. In the present context, spatial random networks might approximate a society under various social distancing measures, when people do not travel much. The degree of social distancing can be expressed by the average number of connections per individual. A network where individuals have a relatively large number of connections would correspond to a society that has stopped traveling but is still interacting to a strong degree on a local level. Stricter social distancing measures would correspond to a reduced number of local connections in this network, e.g. due to people staying at home more. This network structure is shown schematically in Figure 2A. At the other end of the spectrum, we consider the scale-free Barabási-Albert network [52], which is characterized by individuals having non-local connections, and a few individuals having a disproportionately large number of connections (Figure 2B). During social distancing, the connections in such a network can be reduced. Between these two scenarios, we consider a third network that we call “hybrid network” (Figure 2C), or a spatial scale-free network. The backbone consists of spatial network connections, with a set of long-range connections superimposed. Details of how these networks were constructed are given in the Supplementary Materials.

For each network type, we start with a given “null network”, which represents the state of society before strict local distancing measures. Stricter social distancing is implemented by randomly cutting network connections by a given percentage, which we can vary. Through this variation, we can consider a range of different intensities with which non-pharmaceutical interventions are implemented.

The infection dynamics on these networks were simulated stochastically with the following algorithm. As in standard SIR models, we distinguish between susceptible individuals, S, infected, I, and recovered, R, individuals that are immune to infection. Every time step, the network was sampled randomly until infected agents were selected M times, where M is the total number of currently infected individuals. For each infected individual that was selected, a death event occurred with probability P_{death}, and a recovery event occurred with a probability P_{rec} (we refer to the probability of death or recovery as the probability of removal, $P_{removal}$=

$P_{death} + P_{rec}$). With a probability P_{inf} x (number of social connections), an infection event was attempted. In this case, one of the connected individuals was chosen randomly for an infection event. If this individual was susceptible, an infection event proceeded. If this individual was either recovered or dead, no infection occurred. We note that in the context of the model, recovered and dead individuals have the same effect: they represent network nodes that are

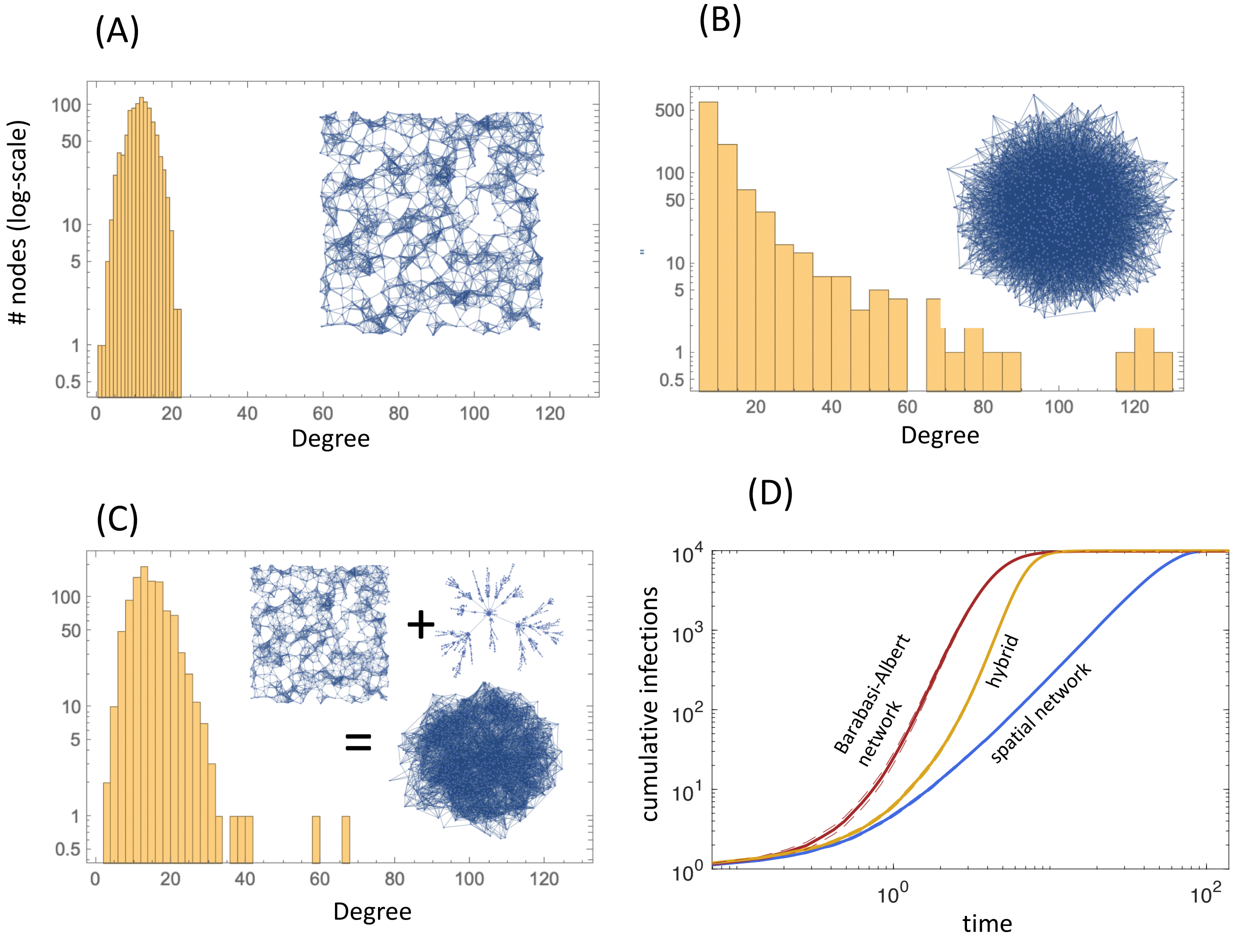

Figure 2: Different network types considered in this paper and their properties (See section 2.1 of the Supplement for details of construction). In (A-C), a typical degree histogram and a graphical representation of a typical network are presented. (A) A random spatial network, where nodes are connected largely to their neighbors, i.e. connections are short-range. (B) Scale-free Barabasi-Albert network, where no spatial correlations are found and there is a power law like tail in the degree distribution. (C) A hybrid network, in which a scale-free component is superimposed onto a spatial component. (D) Growth curves showing the infection spread in the three different networks. Standard errors are shown as dashed lines, which in some cases are too small to see. Parameters were chosen as follows. P_{inf}=0.0001min^{-1} per edge; P_{rec}=0.0001min^{-1}; P_{death}=0.00005min^{-1}.

not available for transmission anymore. We will refer to these individuals as “removed” from the infection process.

Model parameters used here are motivated by the COVID19 epidemic: we select the recovery and death rates based on the literature [12, 53-55] and we use the Method of Simulated Moments (MSM) [56] to calibrate unknown parameters per contact transmission probability to the basic reproduction number R0 and effective reproduction number R_{eff} for COVID19. In our simulations R0 = 3.8, CI = [3.4, 4.2], which is close to that of [12], and the effective reproduction number for when social distancing is implemented by cutting half of the edges is R_{eff} = 1.26, CI = [1.20, 1.32], which is close to that of [53-55].

Basic growth laws

Here, we summarize the infection spread laws observed in the different network models assuming that the networks are in their “null state”, i.e. before connections are cut. The spatial model displays clear power law growth of the infection over time, which is due to the local connections that characterize this network (Figure 2D), see [51, 57-59] for earlier studies of this phenomenon. The scale free Barabási-Albert network displays an initial phase of exponential growth, followed by a transition to a power law, before the final epidemic size has been reached (Figure 2D). This behavior has been analyzed in detail before [34]. The hybrid network displays a similar behavior, although the growth is more skewed towards power law behavior (Figure 2D). Power law growth is not predicted by SIR models that are based on ordinary differential equations, and the observation of power law like spread of COVID19 across different locations [60, 61] thus indicates that network models might be more appropriate descriptions in many settings.

Infection dynamics during social distancing

The network models considered here might shed light onto the mechanism underlying the observed prolonged plateau phenomenon discussed above (Figure 1). We first consider the spatial model. The simulation is started with the "uncut" version of the model that contains 10,000 agents that are characterized by a relatively large number of connections. When the number of infected individuals has reached 100 (1% of the total population), the simulation switches to a strongly cut version of the network, characterized by significantly fewer connections per agent. Figure 3A shows the dynamics averaged over many realizations of the simulation. Implementation of social distancing is followed by a peak of infections, after which the infection levels decline slightly and converge to a long-term plateau, during which average infection levels remain relatively constant. This is also reflected in a linear growth of the cumulative case counts in the simulation (Figure 3B). After a certain period of time at this plateau, the dynamics start to visibly decline. We note that this transition to the decline phase occurs without any further cutting of network connections, i.e. without any further implementation of non-pharmaceutical intervention measures.

These plateau dynamics are explained as follows. When the network is relatively well-connected (pre-social distancing), the infection can spread in two dimensions (Figure 3C),

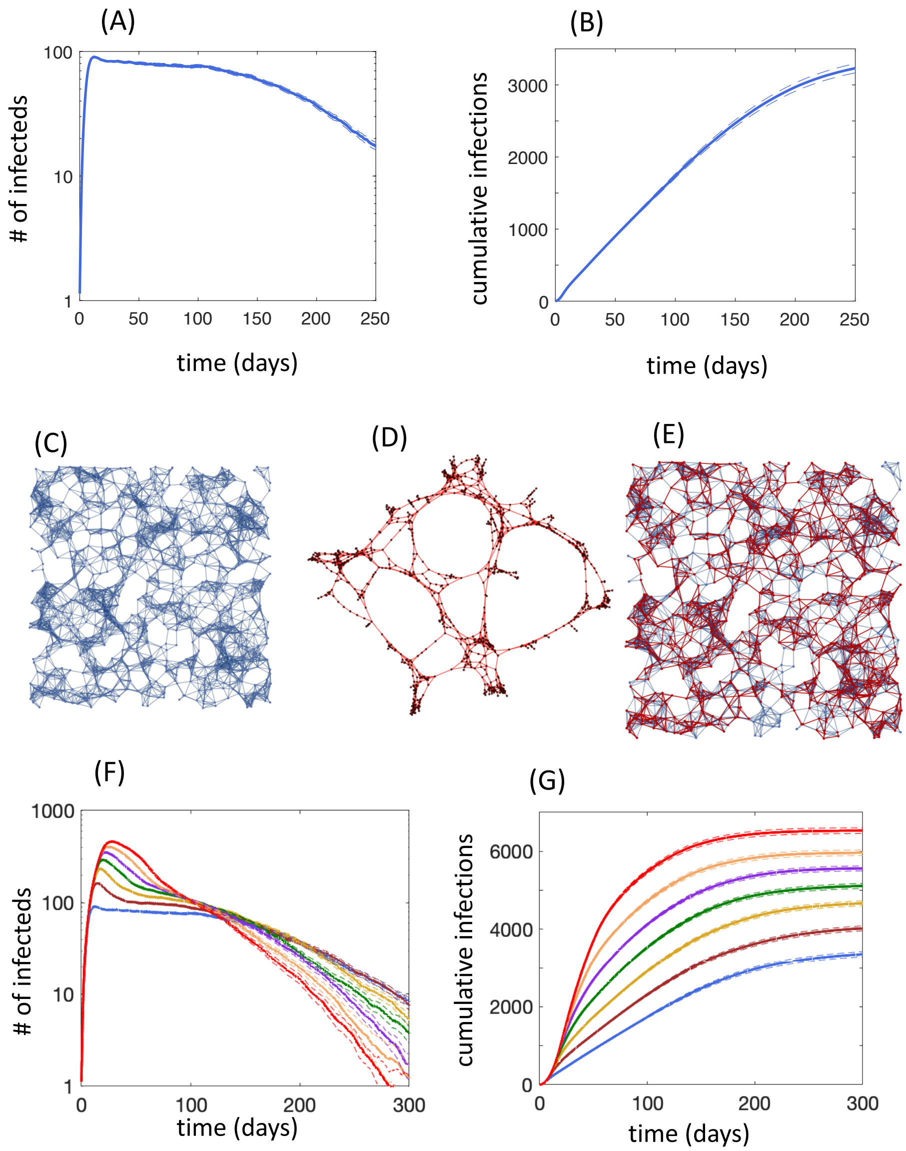

Figure 3. Social distancing dynamics in the spatial network. (A) Growth in the uncut spatial network occurs until 100 infected individuals are present, at which point half of the network connections are randomly removed. The average trajectory over 900 runs is plotted, and standard errors are indicated by dashed lines. A plateau is observed, eventually followed by a decline phase. (B) Same simulation, but cumulative infection numbers are plotted. (C) Schematic illustration of a typical (uncut) spatial network. (D) Schematic illustration of the cut network, which results in the existence of one-dimensional infection corridors. (E) The cut network (red) superimposed onto the uncut network. (F) Same type of simulation as in part (A), but social distancing is initiated when different numbers of infected individuals are reached: 100 (as in part A), 200, 300, 400, 500, 500, 700. These are again averages over 900 simulations, and standard errors are indicated by dashed lines. (G) Same, but cumulative number of infections are plotted. Parameters were as follows. P_{inf}=0.0001min^{-1} per edge; P_{rec}=0.0001min^{-1}; P_{death}=0.00005min^{-1}.

resulting in power law growth, where the number of infections grows quadratically in time, see e.g. the classical results of [58, 59] and more recent results of [51], where a traveling wave solution for a 2D random spatial network predicts a quadratic growth. When the network connections are significantly cut, however, the remaining social pathways along which the infection can spread turn out to be significantly longer, resembling one-dimensional corridors (Figure 3D,E). Infection spread across a one-dimensional graph results in a constant number of new cases per day, as was proven in [51], and is also consistent with results from network models with reduced connections [20]. Although the number of new cases remains roughly constant over time, the infection is still spreading through the community. Over time the infection spread reaches the end of these one-dimensional paths, at which point further spread cannot occur anymore and the infection levels start to decline. Therefore, the plateau phase can be explained by a transition from 2-dimensional to 1-dimensional infection spread, and indicate that the infection is now spreading towards a dead end. In Figures S11, S12, we studied the robustness of the plateau behavior by testing the dynamics for random spatial networks of average degree 10 and 20 [62], under different extent of edge removal (from 10% to 90%). Plateau behavior was observed as long as the extent of edge removal was not too high. In particular, for the spatial network of average degree 10 we observe distinct plateau behavior when between 35% to about 55% of edges are removed; the spatial network of average degree 20 exhibits a plateau when between 65% and 75% of the edges are removed. Figures S8 and S9 further explore parameter dependence of plateau behavior in different networks. In particular, plateau dynamics are not observed for the scale-free Barabási-Albert network which has no spatial component, because upon cutting connections, a transition to a roughly 1-dimensional spread does not happen. As expected, the hybrid network reproduces the plateau behavior, but to a lesser extent than the spatial network (Figure S8).

Figure 3F investigates the timing of the plateau in spatial networks, by showing the dynamics where social distancing is implemented at different percentages of infected individuals, ranging from low to high. Interestingly, we observe that the plateau phase becomes less pronounced the more the infection has spread when social distancing is implemented. For the simulation where social distancing is implemented at the largest percentage of infected individuals, we observe a brief shoulder phase, followed by a relatively rapid decline of infection cases. This is studied further in figure S10, where we explored a more realistic scenario for social distancing. In these simulations, we start with a hybrid network and then, once social distancing is implemented, all (or a large percentage of) long-distance, and a smaller percentage of short-distance edges are removed. We observe that the existence and longevity of the plateau depend on the degree to which the epidemic spreads prior to the start of social distancing. Having long-range connections facilitates the seeding of the infection in different "neighborhoods" of the spatial network. If these infection locations are relatively few and far apart, each of them gives rise to plateau-like dynamics during social distancing, which adds up to a global plateau. If, however, the seeding becomes too dense before the start of social distancing, the spread that continues once the connections are cut leads to the local epidemic outbreaks running into each other and extinguishing each other, resulting in the epidemic exhaustion. This might explain why during the COVID19 pandemic, the plateau tends to be observed only in those locations that started social distancing early enough to prevent extensive infection spread.

Last but not least, the network simulations indicate that immunity of recovered individuals is an essential component of the plateau behavior. This is illustrated in Figure S16, which compares the effect of social distancing on infection spread dynamics in simulations that do and do not assume that recovered individuals are immune, using the spatial network. Without the assumption of immunity, the plateau behavior is not observed, and the number of infected individuals during the phase of social distancing reaches a significantly higher peak (Figure S16). Based on these findings, we hypothesize that the beneficial effect of social distancing is noticeably enhanced by immunity. The reason for this model behavior is that recovered, immune individuals, even if not very prevalent in the population, can provide local roadblocks for infection spread, which contributes to the infection paths being more one-dimensional rather than two-dimensional.

Infection spread upon relaxation of social distancing

Economic considerations require an eventual relaxation of social distancing measures. This enables a resurgence of infection levels, which is also referred to as a second wave. We investigated what our network models predict in this regard. This is a topic that has previously been analyzed with ordinary differential equation SIR models [5, 6]. These studies sought optimal social distancing schedules, where the starting time as well as the extent and duration of social distancing was varied with the aim to find the schedule that minimized over the first and the second peak of infection levels. One finding was that a longer duration of social distancing lowered the peak of the second wave of infection spread following the relaxation of social distancing measures [5, 6]. Similar behavior is also observed in our network models, but added insights can be obtained arising from the existence of the plateau phase when social distancing is implemented. In agreement with the previous work [5, 6], the network models also indicate that a longer duration of social distancing leads to a lower second wave. It does so, however, in a stage-wise manner (Figure 4A,B). While the dynamics are in the plateau phase, a later return to the fully connected network does not significantly decrease the subsequent infection peak (Figure 4A) or the final epidemic size (total number of individuals infected since the beginning of the epidemic, Figure 4B). Once the dynamics have entered the post-plateau decline phase, however, both the infection peak upon return to the fully connected network, as well as the final epidemic size, are noticeably reduced (Figure 4A,B). The model thus gives rise to an important policy suggestion: If plateau-like dynamics are observed during social distancing, it pays off to wait for the transition to the decline phase before relaxing the non-pharmaceutical interventions, such that both future public health burden and economic hardship are reduced.

The reason that the second peak and the final epidemic size are reduced if social distancing is relaxed during the decline phase of the dynamics is that both measures depend on

the population sizes when non-pharmaceutical interventions are reduced, and in particular on the number of infected individuals at this time. Fewer infected individuals lead to a lower peak and a lower final epidemic size, and this is only achieved once the number of infected cases starts to decline during the phase of social distancing. The longer the social distancing phase is

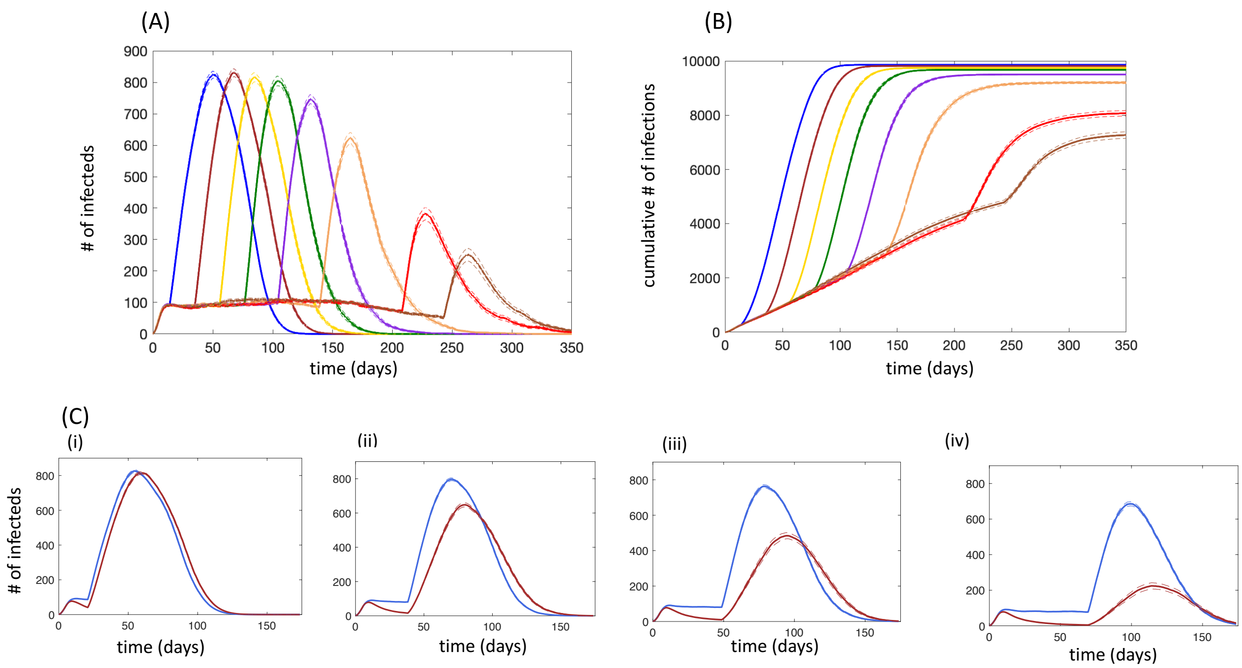

Figure 4. Infection spread dynamics when social distancing is relaxed in the spatial network model. (A) The number of infected individuals is plotted against time. Simulations start with the uncut network. When the infected population reaches size 100, ½ of randomly chosen edges are removed. At different times following the cut, the simulation reverts back to the original network. This results in a renewed wave of spread, and we let the infection spread in the simulation without further network cutting. Generally, a later return to the uncut network leads to a lower peak of the renewed growth. This reduction, however, is very minor, unless the return to the uncut network occurs when the infection levels are already in the decline phase during social distancing. The average over 900 simulations is shown. Standard errors are shown by dashed lines. (B) Same, but cumulative infections over time are shown. (C) Dynamics of the second wave after return to the uncut network, comparing different degrees of social distancing. The blue curve assumes that 50% of the connections are cut during social distancing. The orange curve assumes that 65% of the connections are cut during social distancing, i.e. distancing is stricter. Panels (i) – (iv) show return to the uncut network after longer durations of social distancing. Generally, stricter social distancing leads to a lower peak of the second wave of infections. For final epidemic size, see Figure S10. Each curve represents the average over 900 simulations. Standard errors are shown by dashed lines, which in some cases are too small to see. P_{inf}=0.0001min^{-1} per edge; P_{rec}=0.0001min^{-1}; P_{death}=0.00005min^{-1}.

maintained during this decline, the lower the predicted second peak and the final epidemic size.

We also investigated how the magnitude of the second peak depends on the degree of social distancing, expressed by the degree to which the original network was cut (more cut connections correspond to stricter social distancing). In the spatial network, we find that less strict social distancing results in a higher second peak (Figure 4C) and in a higher final epidemic size (Figure S13), because the number of infected individuals by the end of social distancing is higher if the degree of distancing is less strict.

It is interesting that in SIR models based on ODEs, the opposite is observed: less strict distancing (expressed by a higher rate of infection) results in a lower second peak [5, 6]. The reason is the assumption of perfect mixing in ODE models: less strict distancing leaves fewer individuals uninfected (and hence susceptible), and under a perfect mixing assumption, this significantly slows down the rate of infection spread following the end of social distancing. In the spatial network model, in contrast, the total number of uninfected individuals is less important due to limited connections in this model, and the number of infected individuals when social distancing ends is the main driving factor. Since a higher degree of mixing occurs in the scale-free Barabási-Albert network (compared to the spatial network), the magnitude of the second peak depends in the same way on the degree of distancing as in the ODEs (Figure S14). The hybrid network displays intermediate behavior (Figure S15), where the relationship between the degree of distancing and the second peak depends on the timing of relaxation. If relaxation occurs relatively early, less distancing results in a lower second wave, similar as observed in ODE models. If relaxation occurs later, however, the relationship between the degree of distancing and the predicted second wave is non-monotonic (Figure S15).

Discussion and Conclusion

We have used network models to interpret the dynamics of COVID19 spread during and after social distancing measures. The network models can account for several specific observations. They predict that the infection spreads according to a power law, and further predict the presence of a prolonged plateau phase following the start of non-pharmaceutical intervention measures, if those are implemented relatively early during the epidemic. According to the network models, the plateau occurs because during strict social distancing, infection spread follows nearly one-dimensional transmission corridors, compared to spread in two dimensions before distancing. Another interesting finding was that according to the model, the plateau phase naturally transitions into a decline phase without any further increase in non-pharmaceutical intervention measures. If these are the dynamics that are happening in our communities, then a significant benefit can be achieved if the end of social distancing occurs once the dynamics are already in the decline phase. A premature end of interventions can lead to a higher second wave and a larger final epidemic size.

The network models further indicate that the time at which the interventions are initiated plays an important role, and this is supported by data. The plateau is predicted to be observed if social distancing measures are implemented early (such as in West Coast states), and it is predicted to be much less pronounced if those interventions are started later (such as in New York). This insight might add to our understanding of the heterogeneity in responses to social distancing measures that are found when comparing different locations.

Another interesting observation concerned the role of immunity for the success of social distancing. In our computer simulations, the plateau is only observed if we assume that recovered individuals are immune. In the absence of this assumption, the plateau dynamics are not observed and infection levels during non-pharmaceutical intervention measures are predicted to be significantly higher. Conclusive data about the level of protection in recovered individuals are currently not available.

Our results further emphasize some important differences between ODE and network-based modeling. While the traditional SIR ODE modeling paradigm is capable of reproducing many features of network infection dynamics, some aspects are not captured by the simplified ODE framework. For example, ODE models suggest that the lower the infectivity parameter during the intervention, the higher the second infection wave and the resulting final epidemic size. This result is a consequence of the complete mixing assumption and it is weakened or disappears under a network modeling approach.

It is important to note that model results depend on model assumptions and that uncertainties remain in this regard. While we think that network models are more realistic descriptions of infection spread during non-pharmaceutical interventions than ordinary differential equations that assume perfect mixing, uncertainty remains about the exact contact structure in our societies, which can also differ from location to location (e.g. comparing urban with rural areas). It appears, however, that our results depend on the notion that cutting network connections can transform virus spread in 2 dimensions towards spread paths that are more one-dimensional in nature. It might be possible to test this notion with more detailed data on human contacts during social distancing.

Another source of uncertainty comes from the data that we are interpreting. While a wealth of information exists about confirmed COVID190 case counts in the US and around the world, these counts depend on testing levels, making it hard to compare different locations. The observation that a plateau is observed could in principle also be explained by the limited availability of tests as true infection levels rise. This is unlikely to be the case, however, given that the percent of positive tests is typically not near saturation.

The explanation of the plateau behavior proposed in this paper is not the only possible mechanism of this phenomenon. In [63] it is proposed that plateau behavior might be a consequence of unusual initial conditions (many seeds initiating the infection dynamics) in a near-critical regime under the SIR model. In [64], a very different explanation is proposed which is related to the behavioral changes driven by fatality awareness, where individual protective measures increase with death rates. Each of these proposed mechanisms, including the one presented here, can explain some parts of the complex dynamics observed during the

COVID19 pandemic. It is currently not possible to say which explanation is "the correct one", and it is likely that these dynamics have several underlying mechanisms. The mechanism proposed here has the advantage of relating the plateau behavior with centrally mandated social distancing measures (that usually precede the plateau) and puts forward an explanation of the New York type (``peak and decay") dynamics vs the California type (a prolonged plateau) dynamics in the context of the timing of non-pharmaceutical interventions.

References

[1] Velavan, T.P. & Meyer, C.G. 2020 The COVID-19 epidemic. *Tropical medicine & international health* **25**, 278.

[2] Lewnard, J.A. & Lo, N.C. 2020 Scientific and ethical basis for social-distancing interventions against COVID-19. *The Lancet. Infectious diseases*.

[3] Ferguson, N., Laydon, D., Nedjati Gilani, G., Imai, N., Ainslie, K., Baguelin, M., Bhatia, S., Boonyasiri, A., Cucunuba Perez, Z. & Cuomo-Dannenburg, G. 2020 Report 9: Impact of non-pharmaceutical interventions (NPIs) to reduce COVID19 mortality and healthcare demand.

[4] Fowler, J.H., Hill, S.J., Levin, R. & Obradovich, N. 2020 The effect of stay-at-home orders on COVID-19 infections in the United States. *arXiv preprint arXiv:2004.06098*.

[5] Morris, D.H., Rossine, F.W., Plotkin, J.B. & Levin, S.A. 2020 Optimal, near-optimal, and robust epidemic control. *arXiv preprint arXiv:2004.02209*.

[6] Ngonghala, C.N., Iboi, E., Eikenberry, S., Scotch, M., MacIntyre, C.R., Bonds, M.H. & Gumel, A.B. 2020 Mathematical assessment of the impact of non-pharmaceutical interventions on curtailing the 2019 novel Coronavirus. *Mathematical biosciences*, 108364.

[7] Kucharski, A.J., Russell, T.W., Diamond, C., Liu, Y., Edmunds, J., Funk, S., Eggo, R.M., Sun, F., Jit, M. & Munday, J.D. 2020 Early dynamics of transmission and control of COVID-19: a mathematical modelling study. *The lancet infectious diseases*.

[8] Peng, L., Yang, W., Zhang, D., Zhuge, C. & Hong, L. 2020 Epidemic analysis of COVID-19 in China by dynamical modeling. *arXiv preprint arXiv:2002.06563*.

[9] Peak, C.M., Kahn, R., Grad, Y.H., Childs, L.M., Li, R., Lipsitch, M. & Buckee, C.O. 2020 Modeling the comparative impact of individual quarantine vs. active monitoring of contacts for the mitigation of COVID-19. *medRxiv*.

[10] Jewell, N.P., Lewnard, J.A. & Jewell, B.L. 2020 Predictive mathematical models of the COVID-19 pandemic: Underlying principles and value of projections. *Jama* **323**, 1893-1894.

[11] Holmdahl, I. & Buckee, C. 2020 Wrong but useful—what covid-19 epidemiologic models can and cannot tell us. *New England Journal of Medicine*.

[12] Gatto, M., Bertuzzo, E., Mari, L., Miccoli, S., Carraro, L., Casagrandi, R. & Rinaldo, A. 2020 Spread and dynamics of the COVID-19 epidemic in Italy: Effects of emergency containment measures. *Proceedings of the National Academy of Sciences* **117**, 10484-10491.

[13] Vespignani, A., Tian, H., Dye, C., Lloyd-Smith, J.O., Eggo, R.M., Shrestha, M., Scarpino, S.V., Gutierrez, B., Kraemer, M.U. & Wu, J. 2020 Modelling COVID-19. *Nature Reviews Physics*, 1-3.

[14] Wu, J.T., Leung, K. & Leung, G.M. 2020 Nowcasting and forecasting the potential domestic and international spread of the 2019-nCoV outbreak originating in Wuhan, China: a modelling study. *The Lancet* **395**, 689-697.

[15] Kissler, S.M., Tedijanto, C., Lipsitch, M. & Grad, Y. 2020 Social distancing strategies for curbing the COVID-19 epidemic. *medRxiv*.

[16] Prem, K., Liu, Y., Russell, T.W., Kucharski, A.J., Eggo, R.M., Davies, N., Flasche, S., Clifford, S., Pearson, C.A. & Munday, J.D. 2020 The effect of control strategies to reduce social mixing on outcomes of the COVID-19 epidemic in Wuhan, China: a modelling study. *The Lancet Public Health*.

[17] Giordano, G., Blanchini, F., Bruno, R., Colaneri, P., Di Filippo, A., Di Matteo, A. & Colaneri, M. 2020 Modelling the COVID-19 epidemic and implementation of population-wide interventions in Italy. *Nature medicine*, 1-6.
[18] Block, P., Hoffman, M., Raabe, I.J., Dowd, J.B., Rahal, C., Kashyap, R. & Mills, M.C. 2020 Social network-based distancing strategies to flatten the COVID-19 curve in a post-lockdown world. *Nature Human Behaviour*, 1-9.
[19] Chinazzi, M., Davis, J.T., Ajelli, M., Gioannini, C., Litvinova, M., Merler, S., y Piontti, A.P., Mu, K., Rossi, L. & Sun, K. 2020 The effect of travel restrictions on the spread of the 2019 novel coronavirus (COVID-19) outbreak. *Science* **368**, 395-400.
[20] Thurner, S., Klimek, P. & Hanel, R. 2020 A network-based explanation of why most COVID-19 infection curves are linear. *Proceedings of the National Academy of Sciences* **117**, 22684-22689.
[21] Zhang, J., Litvinova, M., Liang, Y., Wang, Y., Wang, W., Zhao, S., Wu, Q., Merler, S., Viboud, C. & Vespignani, A. 2020 Changes in contact patterns shape the dynamics of the COVID-19 outbreak in China. *Science*.
[22] Wu, Q., Fu, X., Small, M. & Xu, X.-J. 2012 The impact of awareness on epidemic spreading in networks. *Chaos: an interdisciplinary journal of nonlinear science* **22**, 013101.
[23] Barrett, C.L., Bisset, K., Chen, J., Eubank, S., Lewis, B., Kumar, V.A., Marathe, M.V. & Mortveit, H.S. 2009 Interactions among human behavior, social networks, and societal infrastructures: A case study in computational epidemiology. In *Fundamental problems in computing* (pp. 477-507, Springer.
[24] Funk, S., Gilad, E., Watkins, C. & Jansen, V.A. 2009 The spread of awareness and its impact on epidemic outbreaks. *Proceedings of the National Academy of Sciences* **106**, 6872-6877.
[25] Maharaj, S. & Kleczkowski, A. 2012 Controlling epidemic spread by social distancing: Do it well or not at all. *BMC Public Health* **12**, 679.
[26] Leung, K.Y., Ball, F., Sirl, D. & Britton, T. 2018 Individual preventive social distancing during an epidemic may have negative population-level outcomes. *Journal of The Royal Society Interface* **15**, 20180296.
[27] Azizi, A., Montalvo, C., Espinoza, B., Kang, Y. & Castillo-Chavez, C. 2020 Epidemics on networks: Reducing disease transmission using health emergency declarations and peer communication. *Infectious Disease Modelling* **5**, 12-22.
[28] Nishi, A., Dewey, G., Endo, A., Neman, S., Iwamoto, S.K., Ni, M.Y., Tsugawa, Y., Iosifidis, G., Smith, J.D. & Young, S.D. 2020 Network interventions for managing the COVID-19 pandemic and sustaining economy. *Proceedings of the National Academy of Sciences*.
[29] Keeling, M.J. & Eames, K.T. 2005 Networks and epidemic models. *Journal of the Royal Society Interface* **2**, 295-307.
[30] Keeling, M. 2005 The implications of network structure for epidemic dynamics. *Theoretical population biology* **67**, 1-8.
[31] Ferrari, M.J., Bansal, S., Meyers, L.A. & Bjørnstad, O.N. 2006 Network frailty and the geometry of herd immunity. *Proceedings of the Royal Society B: Biological Sciences* **273**, 2743-2748.
[32] Odor, G. 2013 Rare regions of the susceptible-infected-susceptible model on Barabási-Albert networks. *Physical Review E* **87**, 042132.

[33] Barthélemy, M., Barrat, A., Pastor-Satorras, R. & Vespignani, A. 2005 Dynamical patterns of epidemic outbreaks in complex heterogeneous networks. *Journal of theoretical biology* **235**, 275-288.
[34] Vazquez, A. 2006 Polynomial growth in branching processes with diverging reproductive number. *Physical review letters* **96**, 038702.
[35] Block, P., Hoffman, M., Raabe, I.J., Dowd, J.B., Rahal, C., Kashyap, R. & Mills, M.C. 2020 Social network-based distancing strategies to flatten the COVID 19 curve in a post-lockdown world. *arXiv preprint arXiv:2004.07052*.
[36] Bansal, S., Grenfell, B.T. & Meyers, L.A. 2007 When individual behaviour matters: homogeneous and network models in epidemiology. *Journal of the Royal Society Interface* **4**, 879-891.
[37] Nakamaru, M. & Levin, S.A. 2004 Spread of two linked social norms on complex interaction networks. *Journal of theoretical biology* **230**, 57-64.
[38] Diekmann, O. & Heesterbeek, J.A.P. 2000 *Mathematical epidemiology of infectious diseases: model building, analysis and interpretation*, John Wiley & Sons.
[39] Lloyd, A.L., Valeika, S. & Cintrón-Arias, A. 2006 Infection dynamics on small-world networks. *Contemporary Mathematics* **410**, 209-234.
[40] May, R.M. & Lloyd, A.L. 2001 Infection dynamics on scale-free networks. *Physical Review E* **64**, 066112.
[41] Lloyd, A.L. & May, R.M. 2001 How viruses spread among computers and people. *Science* **292**, 1316-1317.
[42] Kiss, I.Z., Miller, J.C. & Simon, P.L. 2017 Mathematics of epidemics on networks. *Cham: Springer* **598**.
[43] Thomas, L.J., Huang, P., Yin, F., Luo, X.I., Almquist, Z.W., Hipp, J.R. & Butts, C.T. 2020 Spatial Heterogeneity Can Lead to Substantial Local Variations in COVID-19 Timing and Severity. *arXiv preprint arXiv:2005.09850*.
[44] Penrose, M. 2003 *Random geometric graphs*, Oxford university press.
[45] Barrat, A., Barthélemy, M. & Vespignani, A. 2005 The effects of spatial constraints on the evolution of weighted complex networks. *Journal of Statistical Mechanics: Theory and Experiment* **2005**, P05003.
[46] Barthélemy, M. 2011 Spatial networks. *Physics Reports* **499**, 1-101.
[47] Ducruet, C. & Beauguitte, L. 2014 Spatial science and network science: review and outcomes of a complex relationship. *Networks and Spatial Economics* **14**, 297-316.
[48] Isham, V., Kaczmarska, J. & Nekovee, M. 2011 Spread of information and infection on finite random networks. *Physical review E* **83**, 046128.
[49] Mollison, D. 1977 Spatial contact models for ecological and epidemic spread. *Journal of the Royal Statistical Society: Series B (Methodological)* **39**, 283-313.
[50] Grenfell, B.T., Bjørnstad, O.N. & Kappey, J. 2001 Travelling waves and spatial hierarchies in measles epidemics. *Nature* **414**, 716-723.
[51] Lang, J.C., De Sterck, H., Kaiser, J.L. & Miller, J.C. 2018 Analytic models for SIR disease spread on random spatial networks. *Journal of Complex Networks* **6**, 948-970.
[52] Albert, R. & Barabási, A.-L. 2002 Statistical mechanics of complex networks. *Reviews of modern physics* **74**, 47.

[53] Chintalapudi, N., Battineni, G., Sagaro, G.G. & Amenta, F. 2020 COVID-19 outbreak reproduction number estimations and forecasting in Marche, Italy. *International Journal of Infectious Diseases*.
[54] Maier, B.F. & Brockmann, D. 2020 Effective containment explains subexponential growth in recent confirmed COVID-19 cases in China. *Science* **368**, 742-746.
[55] Li, R., Pei, S., Chen, B., Song, Y., Zhang, T., Yang, W. & Shaman, J. 2020 Substantial undocumented infection facilitates the rapid dissemination of novel coronavirus (SARS-CoV-2). *Science* **368**, 489-493.
[56] McFadden, D. 1989 A method of simulated moments for estimation of discrete response models without numerical integration. *Econometrica: Journal of the Econometric Society*, 995-1026.
[57] Szendroi, B. & Csányi, G. 2004 Polynomial epidemics and clustering in contact networks. *Proceedings of the Royal Society of London. Series B: Biological Sciences* **271**, S364-S366.
[58] Cox, J. & Durrett, R. 1988 Limit theorems for the spread of epidemics and forest fires. *Stochastic processes and their applications* **30**, 171-191.
[59] Durrett, R. 1995 Epidemic models: their structure and relation to data, Vol. 5. (Cambridge university press.
[60] Wodarz, D. & Komarova, N.L. 2020 Patterns of the COVID19 epidemic spread around the world: exponential vs power laws. *medRxiv*.
[61] Li, M., Chen, J. & Deng, Y. 2020 Scaling features in the spreading of COVID-19. *arXiv preprint arXiv:2002.09199*.
[62] Melegaro, A., Jit, M., Gay, N., Zagheni, E. & Edmunds, W.J. 2011 What types of contacts are important for the spread of infections? Using contact survey data to explore European mixing patterns. *Epidemics* **3**, 143-151.
[63] Radicchi, F. & Bianconi, G. 2020 Epidemic plateau in critical SIR dynamics with non-trivial initial conditions. *arXiv preprint arXiv:2007.15034*.
[64] Weitz, J.S., Park, S.W., Eksin, C. & Dushoff, J. 2020 Awareness-driven Behavior Changes Can Shift the Shape of Epidemics Away from Peaks and Towards Plateaus, Shoulders, and Oscillations. *medRxiv*.